HHS Public Access

Author manuscript

Anal Chem. Author manuscript; available in PMC 2022 August 10.

Published in final edited form as:

Anal Chem. 2021 August 10; 93(31): 11025–11032. doi:10.1021/acs.analchem.1c02399.

Mapping Aerosolized Saliva on Face Coverings for Biosensing Applications

Zhicheng Jin[#], **Alec Jorns**[#]
Department of NanoEngineering, University of California, San Diego, La Jolla, California 92093, United States

Wonjun Yim,
Materials Science and Engineering Program, University of California, San Diego, La Jolla, California 92093, United States;

Ryan Wing,
Department of NanoEngineering, University of California, San Diego, La Jolla, California 92093, United States

Yash Mantri
Department of Bioengineering, University of California, San Diego, La Jolla, California 92093, United States

Jiajing Zhou, **Jingcheng Zhou**, **Zhuohong Wu**, **Colman Moore**
Department of NanoEngineering, University of California, San Diego, La Jolla, California 92093, United States;

William F. Penny,
Division of Cardiology, University of California, San Diego, San Diego, California 92161, United States

Jesse V. Jokerst
Department of NanoEngineering, University of California, San Diego, La Jolla, California 92093, United States; Materials Science and Engineering Program and Department of Radiology, University of California, San Diego, La Jolla, California 92093, United States;

Abstract

Facemasks in congregate settings prevent the transmission of SARS-CoV-2 and help control the ongoing COVID-19 global pandemic because face coverings can arrest transmission of respiratory droplets. While many groups have studied face coverings as personal protective

Corresponding Author: **Jesse V. Jokerst** – Department of NanoEngineering, University of California, San Diego, La Jolla, California 92093, United States; Materials Science and Engineering Program and Department of Radiology, University of California, San Diego, La Jolla, California 92093, United States; jjokerst@ucsd.edu.
[#]Z.J. and A.J. contributed equally to this work.

Supporting Information
The Supporting Information is available free of charge at https://pubs.acs.org/doi/10.1021/acs.analchem.1c02399.
Materials, instrumentations, methods, EBC collection, strip assembly, the recovery of amylase, table of amylase level, and SEM images (PDF)

Complete contact information is available at: https://pubs.acs.org/10.1021/acs.analchem.1c02399

The authors declare no competing financial interest.

equipment, these respiratory droplets can also serve as a diagnostic fluid to report on health state; surprisingly, studies of face coverings from this perspective are quite limited. Here, we determined the concentration and distribution of aerosolized saliva (*via* α-amylase levels) captured on various face coverings. Our results showed that α-amylase accumulated on face coverings in a time-dependent way albeit at different levels, *e.g.*, neck gaiters and surgical masks captured about 3-fold more α-amylase than cloth masks and N95 respirators. In addition, the saliva aerosols were primarily detected on the inner layer of multilayered face coverings. We also found that the distribution of salivary droplets on the mask correlated with the morphologies of face coverings as well as their coherence to the face curvature. These findings motivated us to extend this work and build multifunctional sensing strips capable of detecting biomarkers *in situ* to create "smart" masks. The work highlights that face coverings are promising platforms for biofluid collection and colorimetric biosensing, which bode well for developing surveillance tools for airborne diseases.

Graphical Abstract

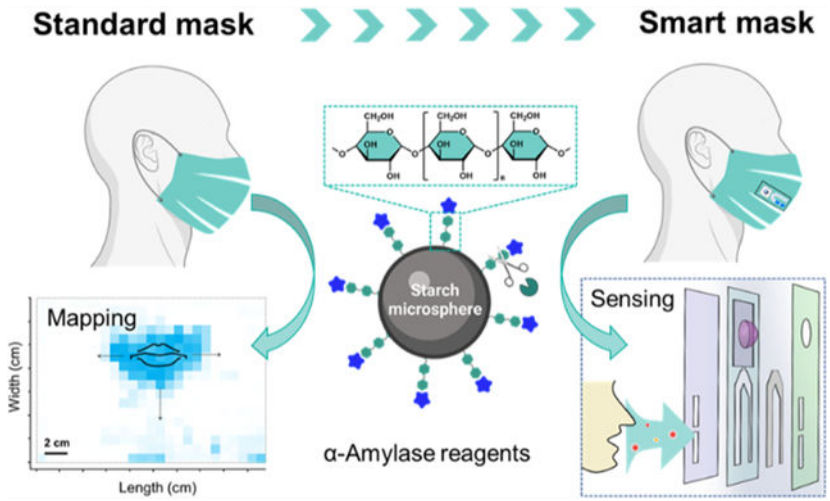

INTRODUCTION

The COVID-19 pandemic is caused by the SARS-CoV-2 virus transmitted *via* aerosols or droplets expelled by speaking, breathing, or coughing.[1,2] Non-pharmacological interventions (*e.g.*, mask-wearing and diagnostic testing) have been crucial in preventing the ongoing spread of SARS-CoV-2 prior to vaccine deployments.[3,4] A continuous poll by YouGov showed that the use of face coverings in public by Americans was 75–80% in early 2021.[5] Face coverings naturally accumulate the exhaled saliva and other aerosolized droplets from the oral cavity.[2,4] Therefore, it is possible that they could offer both protective and diagnostic features when repurposed with analytical capabilities. That is, the exhaled respiratory droplets harbor diagnostic biomarkers (*e.g.*, metabolites, hormones, enzymes, and toxins) that could be harvested from the face coverings and then used to test the wearer's health status.[6–9] For example, pathogenic nucleic acid and viral protease antibodies have recently been found in saliva droplets collected from COVID-19-positive patients.[10,11] While many studies have evaluated the impact of face coverings in reducing transmission with extensive modeling of the distribution of aerosolized droplets, there is limited empirical

data on the accumulation of these droplets on face coverings and the biomarkers contained within.[12,13]

Here, we demonstrated that standard face coverings were effective at capturing the aerosolized saliva droplets. We used a colorimetric test to quantify a canonical salivary biomarker (*i.e.*, α-amylase) and mapped the accumulation of respiratory droplets on four types of face coverings. We then studied the effects of varying a few key parameters (*e.g.*, mask morphology, structural layers, wear-time, and expiratory activities) on the amylase accumulation on mask surfaces. We found that neck gaiters and surgical masks contain 3-fold more α-amylase than N95 respirators. The α-amylase was primarily detected on the inner layer of multilayered masks. Not surprisingly, longer wear-time increases the accumulation of amylase on facemasks. We further validated this concept with a diagnostic test strip that reports the presence of α-amylase colorimetrically.

EXPERIMENTAL SECTION

Participants were aged 23 to 40 years. The work described in this contribution for development of a smart mask was done in preparation for a clinical trial approved by the University of California, San Diego Institutional Review Board. Participants were asked to wear masks under the conditions below:

- **i.** *Mask type*. Participants (n = 5) wore one of the four facial coverings for 8 h: neck gaiter (Anstronic), cloth mask (Port Authority Clothing), surgical mask (Albatross MFG), and N95 respirator (Kimtech, model 53358). Each of these mask types was comparable to the facial covering that the participants wore routinely as a component of personal protective equipment.
- **ii.** *Mask layer*. Participants (n = 5) wore a triple-layered surgical mask for 8 h.
- **iii.** *Time effects*. Participants (n = 5) wore a new neck gaiter for 1, 4, 8, and 16 h.
- **iv.** *Expiratory activities*. Participants (n = 5) completed the following three activities for 1 h each with a fresh neck gaiter: breathing (gentle breathing without opening the mouth), talking (take turns reading a poker card deck at an intermediate and comfortable volume), running (gentle running outdoors at a speed of ~ 5 km/h with an average of ~ 150 heartbeats/min as recorded by a smartphone).
- **v.** *Mask with sensing strips*. Two of the labeled stickers (see assembly details in Supporting Information) were affixed to each face covering type with one sticker inside the mask near the mouth, and another offset parallel outside the mask. Participants (n = 10) wore all four face covering types with stickers for 8 h each.

Prior to wearing masks under different conditions, the participants were given general instructions on how to complete each task. For example, the neck gaiter was worn as a single layer with nose and mouth position labeled and maintained at the same location during mask-wearing. Participants were encouraged to produce similar levels of expiratory activities except task (iv). All participants wore the mask from 10 a.m. to 6 p.m., *i.e.*, 8 h wear-time. For 16 h of wearing-time, participants wore the mask for two successive days in

8-h segments. In task (v), the inside sensing strip for N95 respirators was placed vertically at the front of the breathing chamber.

RESULTS AND DISCUSSION

Masks for Respiratory Droplets Collection.

The term “respiratory droplets” governs a wide range of the exhaled matrices, including aerosolized saliva droplets (upper airways) and exhaled breath condensate (EBC) (lower airways).[14] Saliva is an integrated mixture of secretions produced by salivary glands, which consists of various biological components highly associated with the metabolic status, physiological stress, and inflammatory and systemic diseases.[6] One of the most common is α-amylase—a digestive enzyme that begins the digestion of dietary starches.[6,15] Its ubiquity and high expression level across populations make it an ideal biomarker to trace aerosolized saliva on face coverings. Ten individuals participated in this study.

Figure 1A,B illustrates the processes of measuring the amount and distribution of α-amylase on the materials based on colorimetric assays. This commercial amylase reagent consists of water-insoluble starch microspheres with blue dye covalently linked to the starch *via* an α-1,4-glucosidic bond.[16] The presence of α-amylase digests the linkages and releases the waterborne blue dye, yielding a quantifiable color signal (Figure 1C,D). For example, Figure 2A indicates that a linear response (R^2 = 0.99) of the α-amylase activities to the optical absorbance at 620 nm was correlated in the range of 200–4000 U/L. The amylase reagent was fully digested when the enzymatic activities were ≥4000 U/L, corresponding to the upper limit of detection (LoD) of this method, Abs_{max} ~ 17. Modifications of the amylase reagent were made for a forensic test through coating a thin layer of such starch-dye complexes on a permeable filter paper, which further enables the visualization of saliva staining on mask surfaces. This is also referred to as a forensic press test.[17] Figure 2C–F and Table 1 show the masks tested in this study: (A) neck gaiters made of 90% polyester and 10% spandex, (B) cotton-based cloth masks, (C) surgical masks primarily consisting of polypropylene, and (D) pouch-style N95 respirators composed of polypropylene, polyester, and nylon materials.[18] Scanning electron microscope (SEM) characterization of the inner layer of each mask is given in Figure 2 and of the other layers is supplemented in Figure S1.

Quantitative Assessment of α-Amylase on Face Coverings.

The α-amylase activity in both saliva and EBC matrixes collected from the participants was first evaluated using the amylase reagent, and the absorbance was tracked at 620 nm. We report the median absorbance ($Abs._{me}$) to represent the amylase activities. Figure 2B indicates that the amylase activities in participants’ saliva ranged from 62 520–77 320 U/L with a median value of 73 333 U/L ($Abs._{me}$ = 11.7). These amylase activities per unit saliva are within the clinical range from 30 000–150 000 U/L.[23] In comparison, no amylase was detected in the EBC. We, therefore, note that through the entire study, the α-amylase measured on the face coverings comes from the aerosolized saliva rather than EBC. In addition, we compared the α-amylase levels in the saliva from the participants to the commercial pooled human saliva and found no significant difference in their enzymatic activities ($p > 0.05$, Figure S4).

Initial experiments focused on verifying whether the respiratory saliva droplets were present on the face coverings. This was quantified with the effect of mask type, wearing-time, and expiratory activities. First, we varied the type of face coverings from neck gaiter, cloth mask, surgical mask, and N95 respirators. Figure 3A shows the activities of α-amylase on the worn face coverings were: ≥4000 U/L for neck gaiter; 1400 U/L for cloth mask; 3200 U/L for surgical mask; and 800 U/L for N95 respirator. This indicates that α-amylase enzyme was readily detected on all of the worn face coverings regardless of their morphology. For references, we tested the new face coverings following the same protocol and found no amylase activity (≤200 U/L). In the same panel, a closer examination on the cloth mask and N95 respirator type shows that about 3-fold less amylase activity was measured compared to other masks. This is because the cellulose components in cloth mask inhibit the α-amylase activity *via* reversible and nonspecific absorption interactions.[24] Such interactions resulted in extremely low recovery of α-amylase (~10%) on cloth masks during the sampling processes. In comparison, the recovery of α-amylase on neck gaiter, surgical mask, and N95 respirator was ~90, 70, and 50%, respectively (Figure S4). In addition, the pouch-style N95 respirators have a unique cone shape and empty space in front of the mouth. Rather than concentrating the exhaled aerosols on the detection area, the large breathing chamber favors a broad distribution of saliva droplets, therefore lowering the amylase level on any given area to be tested.[12]

The surgical masks used in this study encompass a tri-layer structure, including the outer layer, middle filter, and inner layer. Our previous study has shown that 90% of mask filtration efficiencies are determined by their middle filter layers,[18] while the outer and inner layers were responsible for removing macroscopic particles. This motivated us to explore the amount of released saliva droplets as a function of structural layers. Figure 3B shows that the amylase was present only on the inner layer after 8 h (*i.e.*, 2866 U/L), whereas no enzyme existed on both middle and outer layers (≤200 U/L). A similar trend was observed with other multilayered face coverings.

We then determined the time evolution of respiratory saliva droplets on neck gaiters as a representative face covering. Figure 3C indicates an overall increased level of salivary amylase with elapsed time: 433 U/L for 1 h; 3000 U/L for 4 h; and ≥4000 U/L for 8 and 16 h. The collected amylase at 8 and 16 h showed similar enzymatic activities, which were restricted to the upper threshold of the amylase reagent assay. It was noteworthy that the α-amylase enzyme maintained its bioactivity on the neck gaiter for at least 12 h (Figure S4). Given the standard curve in Figure 2E, we estimated that the neck gaiter over 8 h of wearing yielded at least 3000 U/L or 0.6 U of the total α-amylase. Nonetheless, the amylase levels measured under the same conditions could show large individual-to-individual variation. This has been attributed to other factors related to human physiological conditions, such as hydration level, speaking frequency, and mask fit, to name a few.[25]

Therefore, we further assessed the respiratory droplets on face coverings under three representative expiratory activities: breathing for 1 h (*i.e.*, without mouth opening), talking for 1 h, and running for 1 h. In Figure 3D, the amount of amylase on the worn neck gaiters under breathing conditions was not detectable. This is because the breathing only was unlikely to create aerosolized saliva and contaminate the neck gaiters with amylase. Such a

finding is consistent with the fact that no amylase was measured in EBC matrix (Figure 2F). In comparison, regular talking and running created strong and repeatable outward airstream from the oral cavity, thus leading to substantial amounts of amylase (*e.g.*, 3400 U/L for talking and ≥4000 U/L for running). The measured α-amylase activities on face coverings under tested conditions are summarized in Table S1.

Overall, the standard face coverings are a viable medium for the collection of aerosolized saliva, and several factors such as mask fit, time of wear, and expiratory activities affect the amount of captured saliva. In terms of mask morphology, the neck gaiter or ear-loop style masks have better capabilities for concentrating the oral fluids compared to the pouch-style N95 respirators, most likely due to the proximity of the mouth to the filtering material. Additionally, the salivary droplets were present only on the inner layer surfaces. The amylase biomarker on neck gaiters exhibited a clear time-dependent accumulation manner and was highly related to the performed human activities.

Distribution of α-Amylase on Face Coverings.

We studied the effects of varying mask morphology and wearing-time on the distribution of airborne saliva using amylase forensics test. In Figure 4A–D, the three segments from top to bottom illustrate the amylase map with mouth-print (top), the side-perspective of airflow directed out of the mask (middle),[26] and the edge of mask fitting to the face (bottom). As shown in Figure 4E, we merged three replicates of each distribution with quantifiable area and color intensity.[27] In Figure 4A, the neck gaiter shows that the turbulent jet during regular speech is mostly directed through the front and sideways. Additionally, droplet flow through the bottom was noticeable, presumably because the elastic seal created along the upper face directed airflow downward and into the looser fitting fabric below the nose and chin.[26] The amylase-presenting area on the neck gaiters was about 45 cm^2 with average color intensity of 182 I/cm^2. In Figure 4B, the ear-loop style masks, including cloth and surgical masks concentrated the expelled droplets on the front, and sideways leakage was observed. This is due to the fact that ear loops mount the mask borders to the face curvature with improved fitting. The staining areas were 25 and 56 cm^2 with averaged staining intensities of 169 and 196 I/cm^2, respectively. Mapping N95 type requires the respirator to be opened and flattened, *e.g.*, the edge is depicted in dashed line in Figure 4D. The difference of saliva distribution for the N95 respirator from others is particularly prominent: amylase was detected over a large area (*i.e.*, 156 cm^2) and no leakage of the droplets was observed. This distribution scenario is due to the consistent seal and sizable breathing chamber of the N95 respirator; therefore, no preference on leakage direction was noticed. The wide spread of aerosolized droplets in the N95 chamber resulted in a 2-fold decrease of the color intensity relative to that of other mask types, *e.g.*, 82 vs ~180 I/cm^2. This trend is consistent with their respective amylase level measured based on the amylase reagents (see Figure 3A). Interestingly, we found no detectable amylase residues beyond the mask fit lines in panels A–D (indicated in dashed orange curves), implying that the distribution of the salivary droplets on the face coverings is highly correlated with the mask morphologies as well as their coherence to the face curvature.

Next, we detailed the amylase map presented on the distinct layer of the surgical mask after 8 h of wearing. Figure 4F shows that the amylase-presenting area were ~ 0.5, 10, and 42 cm^2 for the outer, middle, and inner layers, respectively. In addition, the color intensities of these three layers were 4, 31, and 193 I/cm^2, respectively. Contrary to the expectations based on the pore size scenario, where the middle filtration fabric has 10 times smaller porosity than the inner layer (*i.e.*, 260.5 vs 3084.2 μm^2, as shown in Figure S1), more than 96% of the amylases were captured by the inner layer, while the remaining portion was found on the middle layer.[28] This result also corresponds to the initial finding in Figure 3B, suggesting that most of the aerosolized saliva was collected in the inner layer of face coverings. No biomarker was noticed on the outer fabric. Finally, Figure 4G briefly shows that the time of wear affected both the distribution and concentration of saliva droplets on neck gaiters. The amylase-laden areas were 4, 12, 34, and 56 cm^2 with averaged color intensities of 20, 40, 95, and 151 I/cm^2, for 1, 4, 8, and 16 h of wearing, respectively. This indicates that a prolonged wear-time yielded a high amount and broad distribution of the aerosols on face coverings.

Sensing Strip on Face Coverings.

The above insights regarding the distribution of α-amylase inform optimal placement of sensing device on the face coverings and further reveals improvements of mask design to support the biosensor feature. We next integrated the standard face coverings with a custom test strip inspired by a lateral flow assay. This portable device is capable of collecting and detecting oral biomarkers *in situ* on the face coverings, therefore equipping masks with diagnostic function (Figure 5A). The sensing strip construction and function along with materials is given in Table 2 and Supporting Information. After a simple click of the blister pack (P5), the housed reagents are released to interact with the captured biomarkers on the absorbent pad, triggering specific recognition reactions and producing diagnostic signals. Here, we validate this approach for α-amylase.

First, we tested the levels of saliva amylase accumulated on the sensing strips when affixed on each face covering using amylase reagent (Figure 5B). We chose the hydrophilic treated spunbond polyester as the absorbent pad due to its robust structure, high permeability, hydrophilicity, and biomarker compatibility properties. The bioactivities of α-amylase were found to be well preserved on the polyester pad (Figure S4). Figure 5C–F shows the detected amylase level on four types of stickers ($n = 10$). Surprisingly, despite a 95% reduction in the testing area compared to the naked facemasks (0.72 vs 20 cm^2), the test strip placed inside the face coverings still captured enough amylase for detection. For example, the determined amylase levels were 1166 U/L for the strip placed inside the neck gaiter, 533 U/L for that of the cloth mask, and 2200 U/L for the strip inside the surgical mask. When vertically affixed to the N95 chamber, however, the strip had low efficiency of saliva collection (300 U/L). This could arise by the large breathing room dispersing the amylase at a low amount per area. Additionally, the presence of amylase on the inner strips has a good concordance with that of mask controls ($p > 0.05$). No amylase was detected on the strips placed outside the face coverings. Overall, we conclude that the neck gaiters and ear-loop style masks can be upgraded to smart masks by coupling the inner layer with the portable test strip, which readily collects the individual's respiratory aerosols for sensing purposes.

Next, we provided a proof-of-concept example of smart mask with the capability of detecting amylase *in situ*. Here, an extra layer of forensic press paper (P4) was sandwiched underneath the polyester pad in a test trip (see Figure 6A). The blister pack was loaded with deionized water. A mechanistic scheme is illustrated in the inset: The transmitted amylases release the blue dye from the microsphere surfaces to both absorbent pad and forensic paper in the presence of water media, yielding a color change on both the front and back sides of the sticker. Experimentally, this flow cell strip was attached inside a neck gaiter for 8 h. Figure 6B shows that the test line absorbed water after a simple click and changed to blue color on both sides after 10 min at ambient conditions. For reference, the sealed control line without exposure to any oral droplets retained its original color in white. This experimental manifestation of the color change for probing the amylase biomarker supports our hypothesis that standard face coverings are viable media for developing enhanced diagnostics, which possess multiple functions, including individual protection, respiratory droplets collection, and *in situ* diagnosis. Such sensing masks can target other biomarkers by judiciously tuning the recognition agents on the absorbent pad and buffer reservoir. The design of our smart mask device is simple, affordable, and reliable, allowing for rapid and widespread implementation that could improve testing capabilities beyond standard diagnostic methods such as PCR and antibody testing.

CONCLUSIONS AND FUTURE RESEARCH

We showed that standard face coverings are viable media for collecting aerosolized saliva droplets. We have determined the concentration and distribution of aerosolized saliva droplets released on facemasks under varying conditions. Among the four types of face coverings studied, the neck gaiter and surgical masks displayed ~3-fold higher amylase level than that of cloth masks and N95 respirators. In addition, long wearing-time and strenuous activities dramatically increased the amount of saliva droplets on masks. The pattern of the saliva distributions on the face coverings was related to the mask fitting to the face curvature. Neck gaiters guided the exhaled airflow both sideways and downward. Cloth and surgical masks concentrated the aerotowed saliva on the front and showed some sideways leakage. The tight-fitting N95 respirators spread the droplets over the large breathing chamber. Only the inner layer of each mask showed amylase accumulation, meaning that most of the saliva droplets (>96%) were filtered by the inner fabric. Integrating a portable sensing strip enabled the smart mask with multiple functions, including basic protection, biofluid collection, and *in situ* biomarker diagnosis. Our results defined the pattern of respiratory droplets on face coverings and provided informative rationales for designing smart masks, which could be promising surveillance tools for detecting and lowering the spread of airway-transmitted diseases—particularly when saliva-based diagnostics can be incorporated.

Supplementary Material

Refer to Web version on PubMed Central for supplementary material.

ACKNOWLEDGMENTS

The authors thank internal funding from the UC Office of the President (R00RG2515), and the National Institutes of Health (R01 DE031114) for financial support. This work was supported in part by the National Science Foundation Graduate Research Fellowship Program under Grant No. DGE-1650112. C.M. acknowledges support from the Achievement Rewards for College Scientists (ARCS) Foundation. The SEM work was performed in part at the San Diego Nanotechnology Infrastructure (SDNI) of the University of California San Diego, a member of the National Nanotechnology Coordinated Infrastructure (NNCI), which is supported by the National Science Foundation (Grant ECCS-1542148). Parts of the images in Figures 1, 4, and 5 are created with https://BioRender.com/.

REFERENCES

(1). Prather KA; Marr LC; Schooley RT; McDiarmid MA; Wilson ME; Milton DK Science 2020, 370, 303–304.

(2). Leung NHL; Chu DKW; Shiu EYC; Chan K-H; McDevitt JJ; Hau BJP; Yen H-L; Li Y; Ip DKM; Peiris JSM; Seto W-H; Leung GM; Milton DK; Cowling BJ Nat. Med 2020, 26, 676–680. [PubMed: 32371934]

(3). Chan JF-W; Yip CC-Y; To KK-W; Tang TH-C; Wong SC-Y; Leung K-H; Fung AY-F; Ng AC-K; Zou Z; Tsoi H-W; Choi GK-Y; Tam AR; Cheng VC-C; Chan KH; Tsang OT-Y; Yuen K-YJ Clin. Microbiol 2020, 58, No. e00310–20.

(4). Li Y; Liang M; Gao L; Ayaz Ahmed M; Uy JP; Cheng C; Zhou Q; Sun C Am. J. Infect. Control 2020, 49, 900–906. [PubMed: 33347937]

(5). Richter F Majority of Americans Wear a Mask in Public. https://www.statista.com/chart/22347/share-of-us-adults-saying-they-wear-a-mask-whenin-public-places/.

(6). Malamud D Dent. Clin. North Am 2011, 55, 159–178. [PubMed: 21094724]

(7). Chen Y; Zhang Y; Pan F; Liu J; Wang K; Zhang C; Cheng S; Lu L; Zhang W; Zhang Z; Zhi X; Zhang Q; Alfranca G; de la Fuente JM; Chen D; Cui D ACS Nano 2016, 10, 8169–8179. [PubMed: 27409521]

(8). Wallace MAG; Pleil JD Anal. Chim. Acta 2018, 1024, 18–38. [PubMed: 29776545]

(9). Wu D; Zhou J; Creyer MN; Yim W; Chen Z; Messersmith PB; Jokerst JV Chem. Soc. Rev 2021, 50, 4432–4483. [PubMed: 33595004]

(10). Wyllie AL; Fournier J; Casanovas-Massana A; Campbell M; Tokuyama M; Vijayakumar P; Warren JL; Geng B; Muenker MC; Moore AJ; et al. N. Engl. J. Med 2020, 383, 1283–1286. [PubMed: 32857487]

(11). Martínez-Fleta P; Alfranca A; González-Álvaro I; Casasnovas JM; Fernández-Soto D; Esteso G; Cáceres-Martell Y; Gardeta S; Prat S; Valés-Gómez M SARS-Cov-2 cysteine-like protease (Mpro) is immunogenic and can be detected in serum and saliva of COVID-19-seropositive individuals J. Immunol 2020,205, 3130–3140. [PubMed: 33148714]

(12). Dbouk T; Drikakis D Phys. Fluids 2020, 32, 063303.

(13). Zhao M; Liao L; Xiao W; Yu X; Wang H; Wang Q; Lin YL; Kilinc-Balci FS; Price A; Chu L; Chu MC; Chu S; Cui Y Nano Lett. 2020, 20, 5544–5552. [PubMed: 32484683]

(14). See A; Toh ST Head Neck 2020, 42, 1652–1656. [PubMed: 32357381]

(15). Takai N; Yamaguchi M; Aragaki T; Eto K; Uchihashi K; Nishikawa Y Arch. Oral Biol 2004, 49, 963–968. [PubMed: 15485637]

(16). Prakash A; Lewis SE; Hickman DL Lab. Anim 2016, 45, 433–434.

(17). Hedman J; Dalin E; Rasmusson B; Ansell R Forensic Sci. Int.: Genet 2011, 5, 194–198. [PubMed: 20457099]

(18). Yim W; Cheng D; Patel SH; Kou R; Meng YS; Jokerst JV ACS Appl. Mater. Interfaces 2020, 12, 54473–54480. [PubMed: 33253527]

(19). Fischer EP; Fischer MC; Grass D; Henrion I; Warren WS; Westman E Sci. Adv 2020, 6, No. eabd3083. [PubMed: 32917603]

(20). Lindsley WG; Blachere FM; Law BF; Beezhold DH; Noti JD Aerosol Sci. Technol 2021, 55, 449–457.

(21). Rengasamy S; Eimer B; Shaffer RE Ann. Occup. Hyg 2010, 54, 789–798. [PubMed: 20584862]
(22). Konda A; Prakash A; Moss GA; Schmoldt M; Grant GD; Guha S ACS Nano 2020, 14, 6339–6347. [PubMed: 32329337]
(23). Mandel AL; Peyrot des Gachons C; Plank KL; Alarcon S; Breslin PAS PLoS One 2010, 5, No. e13352. [PubMed: 20967220]
(24). Dhital S; Gidley MJ; Warren FJ Carbohydr. Polym 2015, 123, 305–312. [PubMed: 25843863]
(25). Asadi S; Cappa CD; Barreda S; Wexler AS; Bouvier NM; Ristenpart WD Sci. Rep 2020, 10, No. 15665. [PubMed: 32973285]
(26). Tang JW; Liebner TJ; Craven BA; Settles GSJR Soc., Interface 2009, 6, S727–S736. [PubMed: 19815575]
(27). Zhou J; Jokerst JV Photoacoustics 2020, 20, No. 100211. [PubMed: 33163358]
(28). Yang S; Lee GW; Chen CM; Wu CC; Yu KP J. Aerosol Sci 2007, 20, 484–494.

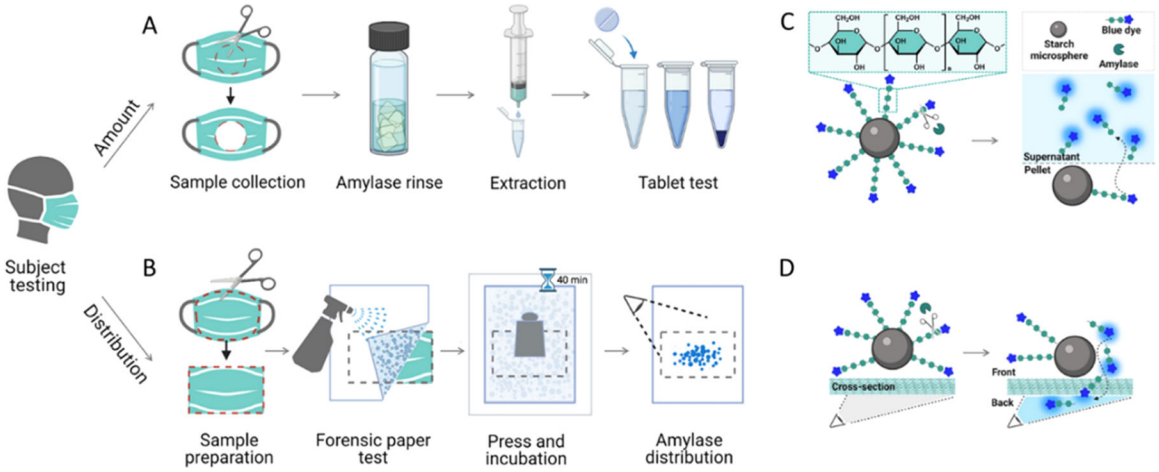

Figure 1.

Schematic illustration of saliva aerosols measurement on face coverings. (A) An amylase reagent for quantifying the activities of α-amylase captured by a mask. (B) A forensic press paper was used to map the distribution of α-amylase on mask surfaces. As shown are the mechanistic representation of the amylase reagent (C) and forensic paper (D) test. α-Amylase digests the α-1,4-glucosidic linkage and releases the blue dyes from the starch microsphere, producing colorimetric signals.

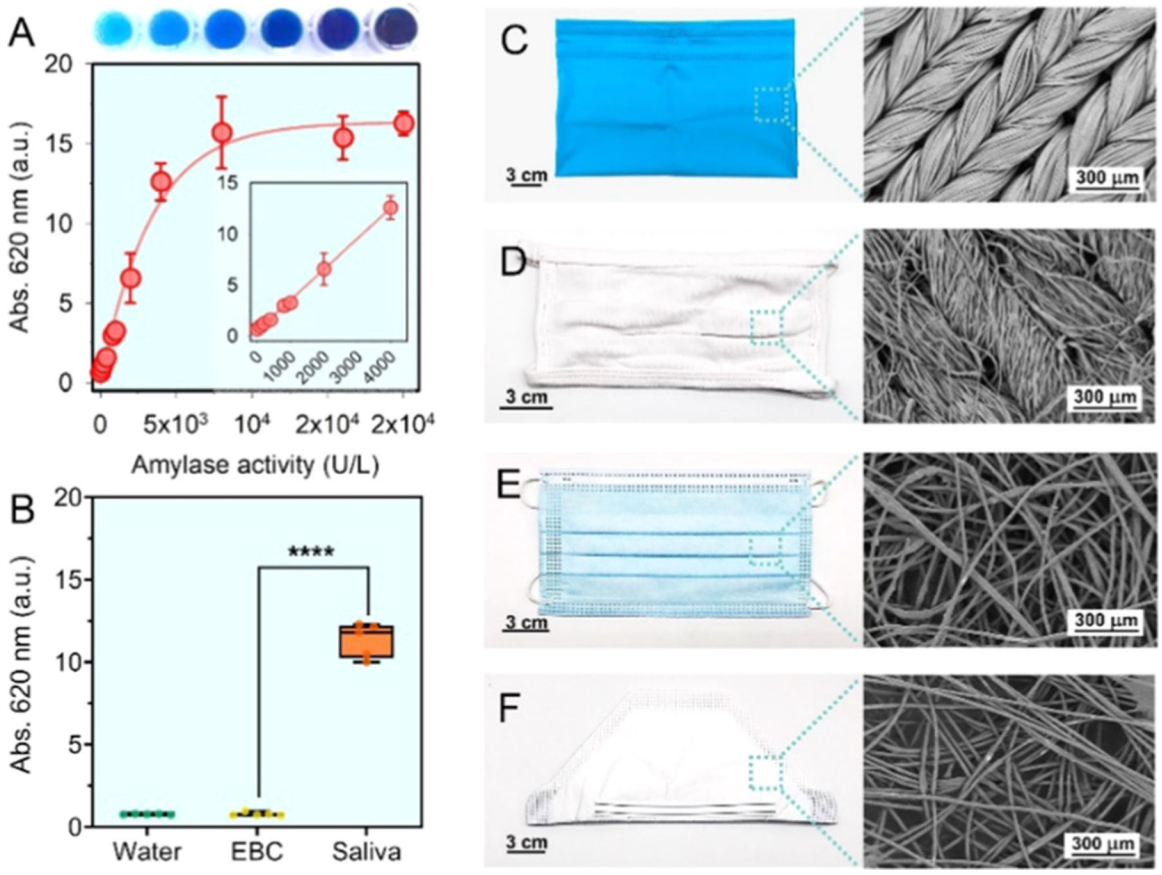

Figure 2.

Appearance, microscopic structures, and amylase detection of the face coverings. (A) The standard curve correlated the α-amylase activities to the optical density at 620 nm (blue color). Inset shows a linear response, with a function of Abs.= 0.7 + 0.003 × activities (in U/L), R^2 = 0.99. (B) Amylase tablet test showed that the saliva contributed the major α-amylase activities (73 333 U/L, $Abs._{me}$ = 11.7), while no amylase (≤200 U/L, $Abs._{me}$ = 0.7) was measured in exhaled breath condensate, EBC (n = 5). (C–F) Neck gaiter, cloth mask, surgical mask, N95 respirator, and the SEM image of their inner fabric.

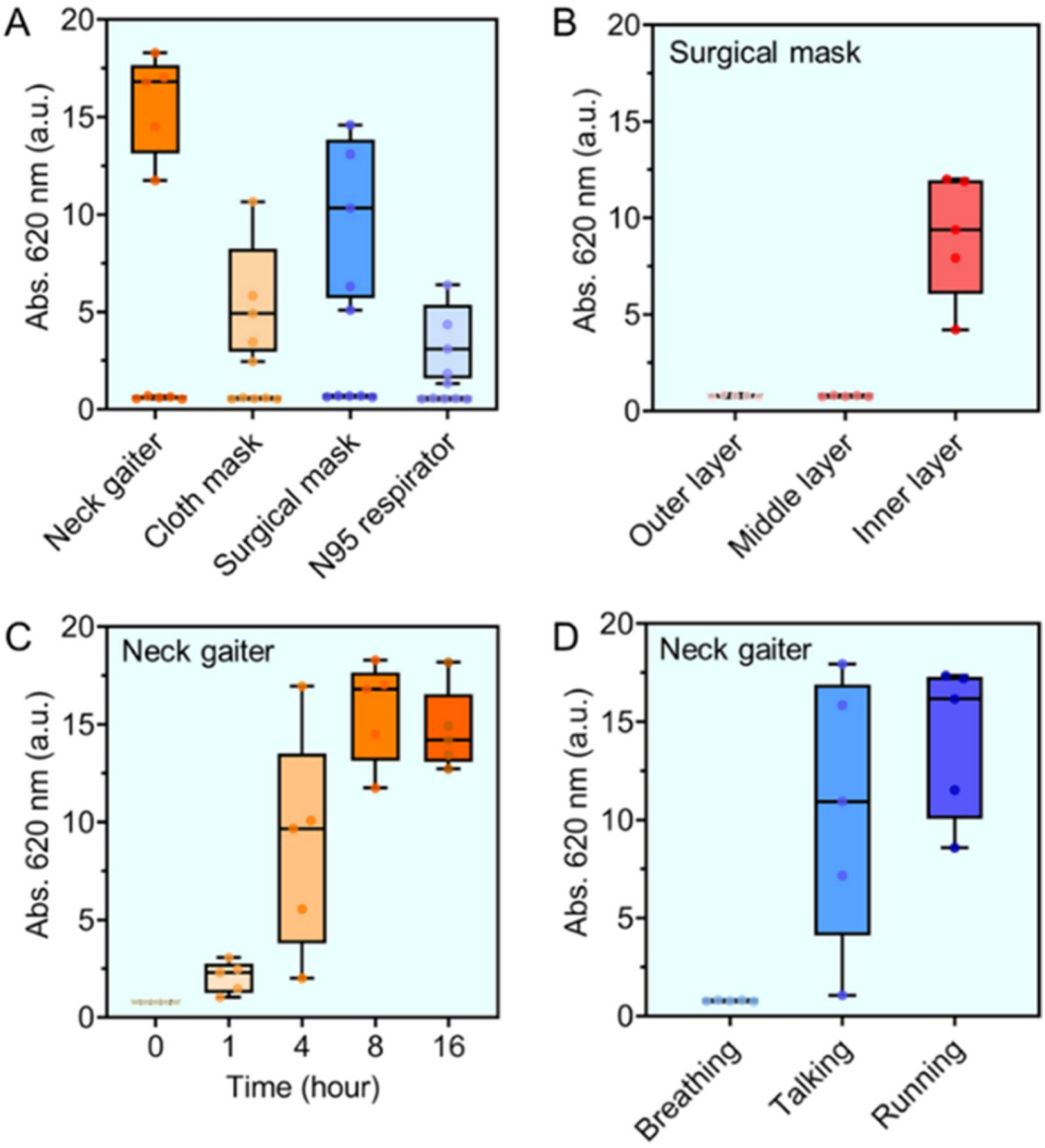

Figure 3.

Quantitative assessment of α-amylase on face coverings. (A) The activities of amylase were: ≥4000 U/L, $Abs._{me}$ = 16.8 for neck gaiter; 1400 U/L, $Abs._{me}$ = 4.9 for cloth mask; 3200 U/L, $Abs._{me}$ = 10.3 for surgical mask; and 800 U/L, $Abs._{me}$ = 3.1 for N95 respirator for 8 h wearing. The new masks contained no amylase activity ($Abs._{me}$ ~ 0.7, see data corresponding to baseline for each). (B) Tri-layer surgical mask shows that the inner fabric captured most of the released salivary amylase (2866 U/L, $Abs._{me}$ = 9.3). No amylase was detected on the middle and outer layers. (C) Time evolution of α-amylase level on neck gaiters. The activities of amylase were: 433 U/L, $Abs._{me}$ = 2.0 for 1 h; 3000 U/L, $Abs._{me}$ = 9.7 for 4 h; ≥4000 U/L, $Abs._{me}$ = 16.8 for 8 h; and ≥4000 U/L, $Abs._{me}$ = 14. 2 for 16 h. (D) The measured amylase amount under representative expiratory activities such as breathing (≤200 U/L, $Abs._{me}$ = 0.7), talking (3400 U/L, $Abs._{me}$ = 10.9), and running (≥4000 U/L, $Abs._{me}$ = 16.1) for 1 h. Data on all panels were from 5 participants (n = 5).

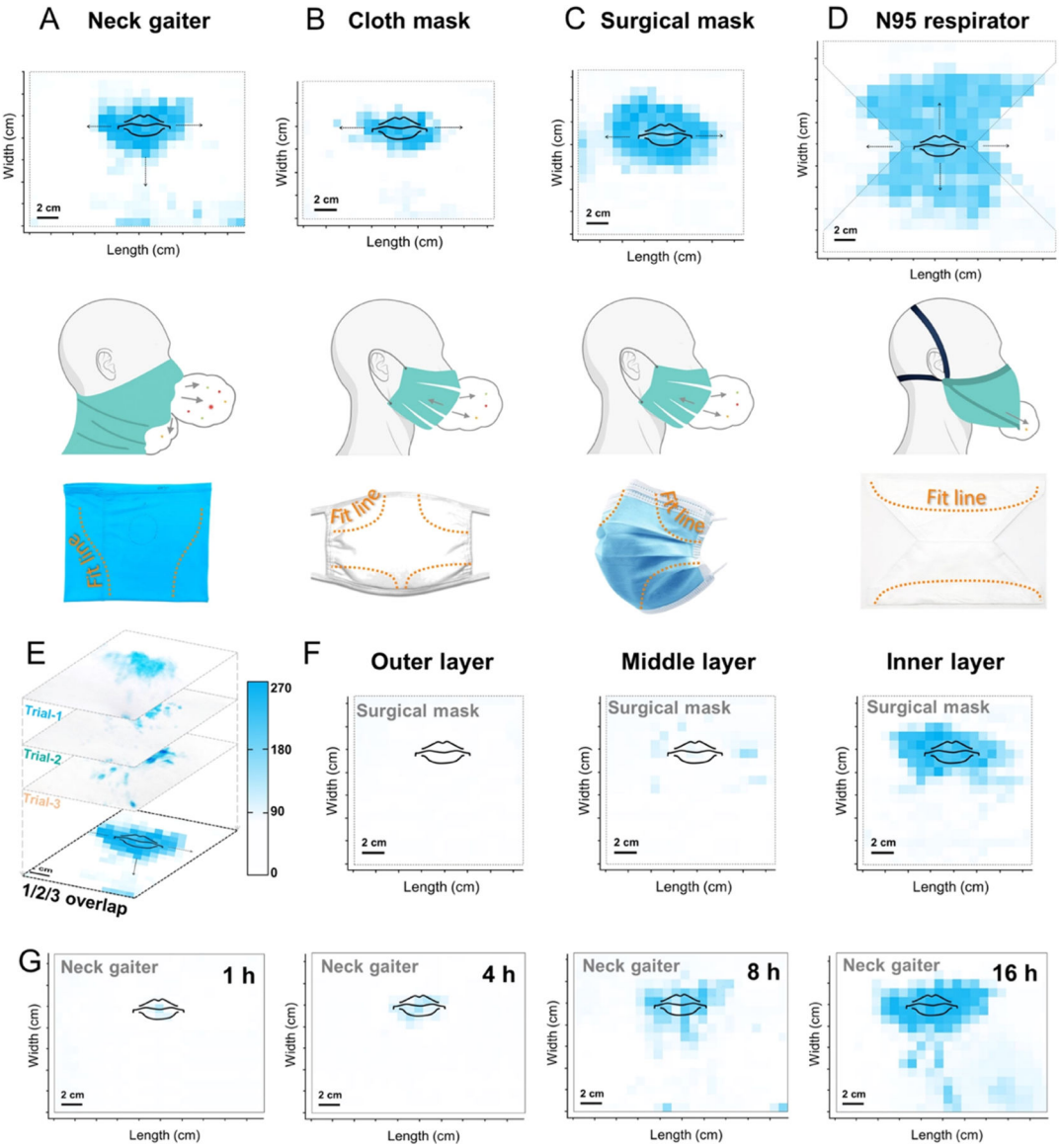

Figure 4.

Distribution of saliva droplets on face coverings. The blue pixels on the map indicate the presence of α-amylase. (A–D) Top panel: amylase distribution on flattened face coverings with a mouth-print. Middle panel: a turbulent jet of respiratory flow. Bottom panel: mask fit to face curvature. Neck gaiter (A) guided the airborne droplets to spread sideways and downward. (E) Each overlayed map counted for three replicates (n = 3, by the same participant). Masks were worn for 8 h, and the inner layer was tested unless otherwise specified. The scale bar designates the color intensity in I/cm^2. (F) Tri-layer surgical mask shows that the inner layer contained significant amylase, while middle and outer fabrics had little to none. (G) Longer time of wear increased the amylase concentration and area on neck gaiters.

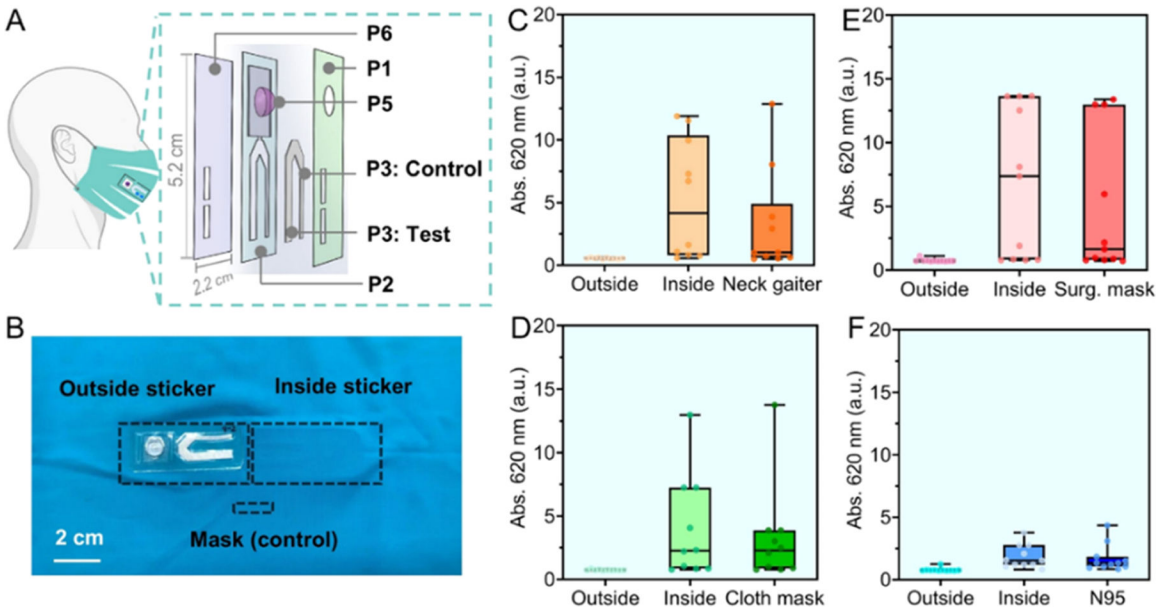

Figure 5.

"Smart" mask combines face coverings and sensing strip. (A) Structural illustration of the flow cell sensing strip. The vents (~0.72 cm^2) on the top cover (P1) and bottom adhesive layer (P6) allowed the transmitted aerosolized saliva to be concentrated on the absorbent pad (P3). The function of other pieces P2, P5 are given in Table 2. (B) A white-light image shows that one test strip was affixed outside the neck gaiter and another offset parallel inside the mask. The mask material of area ~0.72 cm^2 was cropped as a control sample. Participants (n = 10) wore each face covering with strips for 8 h. The measured amylase level on the outside/inside strips attached to different face coverings are shown in panel (C) neck gaiter, (D) cloth mask, (E) surgical mask, and (F) N95 respirator. Data from mask controls were also included. The outside strips contained no amylase activity for all smart masks (≤200 U/L, $Abs._{me}$ ~ 0.7). The inside strips arrested amylase at levels of: 1166 U/L, $Abs._{me}$ = 4.2 for neck gaiter, 533 U/L, $Abs._{me}$ = 2.3 for cloth mask, 2200 U/L, $Abs._{me}$ = 7.4 for surgical mask, and 300 U/L, $Abs._{me}$ = 1.6 for N95 respirator.

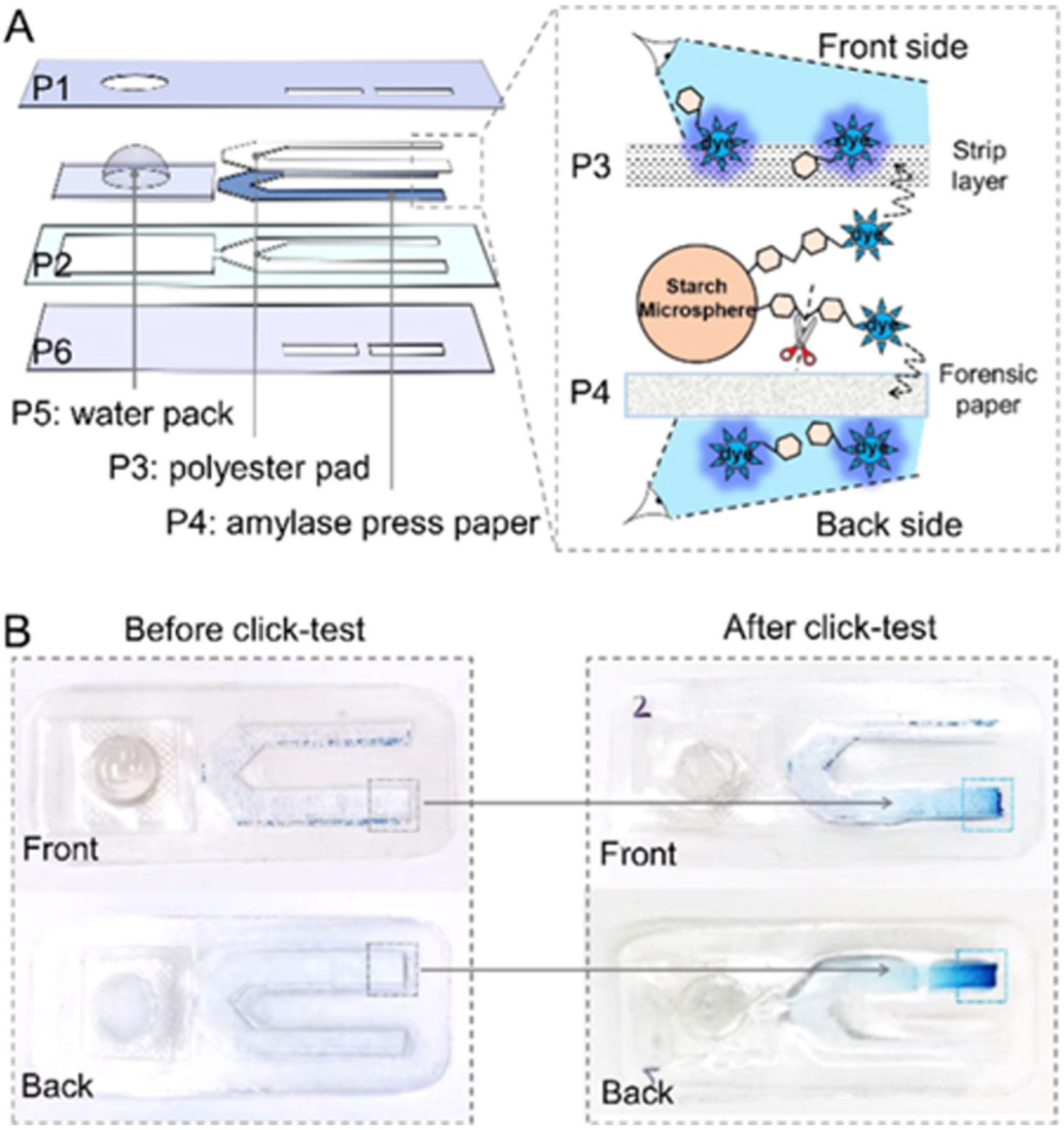

Figure 6.

Smart mask for sensing amylase. (A) Structure of the amylase-sensitive strip. Details for each layer are given in Table 2. The inset shows the detection mechanism. (B) White-light images of the amylase-sensing strip before and after click. The test line on the pad shifted its color from white to blue, which can be viewed from both front and back sides.

Table 1.

Information of the Investigated Face Coverings

face coverings	neck gaiter	cloth mask	surgical mask	N95 respirator
components	90% polyester and 10% spandex	100% cotton	polypropylene[18]	polypropylene, polyester, and nylon materials[18]
style	elastic closure	ear loops	ear loops	pouch, headbands
layer	single	triple	triple	multiple
fabric structure	woven	woven	nonwoven	nonwoven
filtration efficiency	0–40% for 0.6 μm aerosols[19,20]	20–30% for 0.4 μm aerosols[21]	≥90% for 0.3 μm particulates[22]	≥99% for 0.3 μm particles[13,22]
size (cm^2)	24 × 40	16 × 8	17 × 9	24 × 9
manufacturer	anstronic	port authority clothing	Albatross MFG	Kimtech

Table 2.

Structural Components of the Sensing Strip

piece	function	materials	manufacturer
P1	cover	PET carrier film	Drytac Facemount
P2	channel spacer	biaxially oriented PET film	Clear Grafix Dura-Lar
P3	absorbent pad	polyester, grade 6613H	Ahlstrom Munskjo
P4	amylase detection	amylase press paper	Phadebas
P5	reagent storage	clear thermoformed blister pack	Dulcolax
P6	adhesive layer	adhesive PET carrier film	Drytac MultiTac